

Original Research

The protective effects of C16 peptide and angiotensin-1 compound in lipopolysaccharide-induced acute respiratory distress syndrome

Dingqian Wu¹, Xiaoxiao Fu², Yuanyuan Zhang², Qiang Li¹, Ligang Ye¹, Shu Han^{2,*}  and Mao Zhang^{1,*}

¹The Emergency Medicine Department; the Second Affiliated Hospital Zhejiang University School of Medicine (SAHZU), Hangzhou 310058, China; ²Institute of Anatomy and Cell Biology, Medical College, Zhejiang University, Hangzhou 310058, China
Corresponding authors: Shu Han. Email: Han00shu@zju.edu.cn; Mao Zhang. Email: z2jzk@zju.edu.cn

*These authors contributed equally to this paper.

Impact statement

The mixture of C16 peptide and Ang-1 is a novel therapeutic agent, which has been confirmed as effective in several inflammatory diseases of central nervous system in previous studies. Since this compound medicine has a general role in protecting against inflammation and edema, its acting mechanisms may be not tissue- or organ-specific, and it may provide a valuable clue to the potential clinical application in the prevention and treatment of inflammatory lung diseases like ARDS. The experimental research of the novel therapeutic agent's potential protective effects in different animal models will be beneficial for the future drug transformation and clinical trial.

Abstract

C16 peptide and angiotensin-1 (Ang-1) have been found to have anti-inflammatory activity in various inflammation-related diseases. However, their combined role in acute respiratory distress syndrome (ARDS) has not been investigated yet. The objective of this study was to investigate the effects of C16 peptide and Ang-1 in combination with lipopolysaccharide (LPS)-induced inflammatory insult *in vitro* and *in vivo*. Human pulmonary microvascular endothelial cells and human pulmonary alveolar epithelial cells were used as cell culture systems, and an ARDS rodent model was used for *in vivo* studies. Our results demonstrated that C16 and Ang-1 in combination significantly suppressed inflammatory cell transmigration by 33% in comparison with the vehicle alone, and decreased the lung tissue wet-to-dry lung weight ratio to a maximum of 1.53, compared to 3.55 in the vehicle group in ARDS rats. Moreover, C + A treatment reduced the histology injury score to 60% of the vehicle control,

enhanced arterial oxygen saturation (SO₂), decreased arterial carbon dioxide partial pressure (PCO₂), and increased oxygen partial pressure (PO₂) in ARDS rats, while also improving the survival rate from 47% (7/15) to 80% (12/15) and diminishing fibrosis, necrosis, and apoptosis in lung tissue. Furthermore, when C + A therapy was administered 4 h following LPS injection, the treatment showed significant alleviating effects on pulmonary inflammatory cell infiltration 24 h postinsult. In conclusion, our *in vitro* and *in vivo* studies show that C16 and Ang-1 exert protective effects against LPS-induced inflammatory insult. C16 and Ang-1 hold promise as a novel agent against LPS-induced ARDS. Further studies are needed to determine the potential for C16 and Ang-1 in combination in treating inflammatory lung diseases.

Keywords: Acute respiratory distress syndrome, lipopolysaccharide, angiotensin-1, C16, pulmonary inflammation

Experimental Biology and Medicine 2020; 245: 1683–1696. DOI: 10.1177/1535370220953791

Introduction

Acute respiratory distress syndrome (ARDS) is a rapidly progressive disease occurring in patients suffering from significant injuries or critical illness, and it poses a severe threat to human health. ARDS appears as sudden onset of respiratory failure characterized by acute hypoxemia,

pulmonary infiltrates and edema, decreased pulmonary compliance, inflammatory cell infiltration, and gas-exchange abnormality.¹ Despite recent advances in the development of ARDS therapies like anti-inflammatory treatment, ARDS is still one of the leading causes of death in patients who die early. There is an urgent need to identify novel therapeutic strategies against ARDS. Evidence has

shown that ARDS involves major, diffuse injury in the alveolo-capillary wall and increased pulmonary vascular permeability.² Therefore, a potential therapy for ARDS may be achieved by restoring the integrity of the pulmonary endothelial barrier and thus minimizing protein/leukocyte infiltration under ARDS conditions.

Previous studies have demonstrated that the vessel leakage in pulmonary infection and ARDS might be attributed to deregulation of a non-redundant endothelial control pathway triggered by the Tie2 receptor and its ligands, the angiopoietins.³ Therefore, Tie2-activating drugs or agents could play a potential role in leaky vessel repair in ARDS. Our previous studies showed that angiopoietin-1 (Ang-1) promotes angiogenesis and alleviates ischemic injury in the central nervous system (CNS) by interacting with Tie2 predominantly expressed on the endothelial cells (ECs) of blood vessels.^{4,5} In addition, Ang-1 reduces vascular permeability, which is likely due to its ability to maintain the integrity of EC tight junctions under pathological conditions.⁵

On the other hand, C16 peptide (KAFDITYVRLKF), just like Ang-1, can also repair blood vessels by binding to integrins $\alpha v\beta 3$ and $\alpha 5\beta 1$, which promotes EC survival.⁶⁻⁸ The individual roles of C16 and Ang-1 have been well defined in animal models of CNS inflammation in our previous studies.^{4,6-8} In general, the individual application of synthetic C16 peptide inhibits transmigration and infiltration of leukocytes,^{6,7} whereas Ang-1 significantly reduces the blood vessel leakage and diminishes vascular permeability.⁴ Because these two factors act differentially, and their actions are not tissue- or organ-specific, we sought to investigate the combined effects of C16 and Ang-1, rather than their individual effects, on lipopolysaccharide (LPS)-induced pulmonary injury in this study. We hypothesize that C16 and Ang-1 have synergistic effects in suppressing leukocyte/lymphocyte infiltration, protecting ECs from hyperpermeability, and improving the inflammatory microenvironment within the respiratory system.

In the present study, we established a LPS insult injury model in cultured human pulmonary microvascular endothelial cells (HPMECs) and human pulmonary alveolar epithelial cells (HPAEpiCs) as well as a rat model of LPS-induced ARDS, the most commonly used model for inducing acute lung injury. The assumed protective effects of C16 plus Ang-1 were examined *in vitro* and *in vivo*.

Materials and methods

Cell culture

HPMECs and HPAEpiCs and the human monocyte cell line THP-1 were all purchased from American Type Culture Collection (Wesel, Germany). THP-1 cells were maintained in RPMI-1640 (Sigma-Aldrich, St Louis, MO, USA) supplemented with 10% fetal bovine serum (FBS; PAA Laboratories, Linz, Austria) and 20 mM HEPES (Sigma-Aldrich). HPMECs and HPAEpiCs were maintained in Dulbecco's Modified Eagle Medium (Sigma-Aldrich) supplemented with 10% FBS. All cells were grown in a 5% CO₂

humidified atmosphere at 37°C. The medium was refreshed every 2–3 days.

Cell viability assay

HPMECs were plated in 96-well plates at a density of 2×10^4 cells/well and maintained for 24 h at 37°C. Cells were then serum-starved for an additional 24 h, followed by treatment with vehicle (culture medium), LPS (L, 10 μ g/mL) only, or LPS + C16 (C, 600 μ M) + Ang-1 (A, 100 ng/mL) for 24 h.⁵ Then 20 μ L of MTT solution (Sigma-Aldrich, 5 mg/mL in phosphate-buffered saline) was added to the medium at 37°C. Four hours later, the supernatant was replaced with 100 μ L of dimethyl sulfoxide. Optical absorbance was measured at 570 nm in a microplate reader (Multiskan MK3, Thermo Fisher Scientific Inc., Waltham, MA, USA). Cell viability was quantified as the ratio of the absorbance for L- or L + C + A-treated cells to that of the vehicle-treated cells.

Quantification of cell necrosis

Briefly, HPMECs and HPAEpiCs were treated with vehicle or C + A for 24 h, followed by stimulation with 200 ng/mL LPS (Sigma-Aldrich) for 4 h. Hoechst 33342/propidium iodide (PI) double staining was performed as described previously,⁹ and imaged using a Nikon CCD camera E600. The total number of cells and necrotic cells (red) was counted in six randomly selected fields at 400 \times magnification in triplicate. The percentage of necrotic cells was calculated as the number of necrotic cells/the total number of cells $\times 100\%$.

Immunofluorescent staining of apoptotic cells

HPMECs and HPAEpiCs were stimulated with 200 ng/mL LPS for 24 h and then fixed in 4% paraformaldehyde for 30 min followed by incubation with primary mouse polyclonal anti-caspase-3 (cleaved caspase, 1:800; Cayman Chemical, Ann Arbor, MI, USA). Coverslips were rinsed with PBS and incubated with tetramethylrhodamine (TRITC)-conjugated secondary antibodies (1:200; Invitrogen) for 1 h at 37°C, followed by mounting with antifade aqueous mounting media (Southern Biotech, Birmingham, AL, USA) containing 1% Hoechst 33342 nuclear dye (Sigma-Aldrich). Control group were incubated in PBS instead of primary antibodies. The staining was imaged, and the total number of cells and the numbers of doubly positive cells were counted in six randomly selected fields at 400 \times magnification in triplicate. The percentage of apoptotic cells was calculated as the number of doubly stained cells/the total number of cells $\times 100\%$.

Transendothelial migration assay

A leukocyte transmigration assay was performed as described previously.⁵ Briefly, HPMECs were cultured on permeable filters in Transwell culture plates ([®]-96 permeable supports, Costar, Cambridge, MA, USA) at a density of 2×10^4 cells/well, and the HPAEpiCs were added to poly-D-lysine-coated slides in the lower compartments of the Transwells. Cells reached 100% confluency after 72–96 h

of culture. Then 2×10^5 monocytic THP-1 cells were plated onto HPMECs in the inner chamber of the Transwell plates. In vehicle control group, THP-1 cells were allowed to migrate for 6 h at 37°C. In the LPS insult and L + C + A-treated groups, 200 ng/mL LPS was added to the culture medium in the inner chamber. In the C + A- and L + C + A-treated groups, C16 peptide (600 μM) and Ang-1 (100 ng/mL) were added to the medium in the inner chamber to preincubate overnight prior to addition of THP-1 cells. The cells that had transmigrated across the EC layer were counted.

Enzyme-linked immunosorbent assay (ELISA)

In the LPS insult and L + C + A-treated groups, 200 ng/mL LPS were added to the culture medium in the inner chamber; in L + C + A-treated groups, C16 peptide (600 μM) and Ang-1 (100 ng/mL) were also added to the medium in the inner chamber to incubate overnight. The vehicle control was only incubated with culture medium. The inner compartments were removed, and cell culture medium was collected to determine the levels of tumor necrosis factor alpha (TNF-α), interleukin (IL)-1β, IL-8, and IL-10 using ELISA kits (R&D Systems, Minneapolis, MN, USA) in a microplate reader at 450 nm.

In vivo experiments

Animals. A total of 285 adult Wistar rats (male, 250–300 g) were purchased from the Laboratory Animal Center of Zhejiang University and randomly divided into three groups: normal control group (n = 15, no LPS insult), LPS insult (4 mg/kg, iv) only (120 in total, n = 15 at each time point), and L + C + A group (150 in total, n = 15 at 1 and 2 h time points; n = 20 at 4, 6, 12, 24, 72 h, and 1 w time points). ARDS was induced with LPS (L4391, Sigma-Aldrich) by intravenous injection (4 mg/kg) in LPS insult and L + C + A groups, while the LPS group received injection of PBS only. Animal experiments were carried out following the Guide for the Care and Use of Laboratory Animals issued by the National Institutes of Health and approved by the animal ethics committee of Zhejiang University.

Drug administration. The doses of C16 and Ang-1 used in this study were based on the findings of our previous studies on experimental autoimmune encephalomyelitis, an animal model of multiple sclerosis.^{4,8} C16 peptide (KAFDITYVRLKF) was synthesized as previously described^{10,11} and dissolved in PBS at a final concentration of 4 mg/mL. Ang-1 peptide (Shanghai Science Peptide Biological Technology Co., Ltd, Shanghai, China) was dissolved in distilled water at a final concentration of 800 μg/mL.¹² For the rats receiving Ang-1 + C16, 0.5 mL Ang-1 solution and 0.5 mL C16 solution^{7,8} were injected intravenously *via* the caudal vein. For subgroups treated for 1, 2, 4, 6, 12, and 24 h, the injection was administered immediately following LPS insult. In the 72 h and 1 w subgroups, the injection was administered once daily. Rats in the LPS group received intravenous injections of PBS.

In addition, C16 and Ang-1 treatment was given at 6 h postinsult (pi) in 30 rats. The 6 h period was chosen mainly

because this is the time within which diagnosis was made and intravenous treatments could be started.

Arterial blood gas analysis. Arterial blood was collected *via* the abdominal aorta. The pH value, arterial carbon dioxide tension (paCO₂), partial pressure of oxygen (PaO₂), and oxygen saturation (SO₂) were measured automatically using a blood gas analyzer (GEM Premier3000, MA).

Bronchoalveolar lavage fluid (BALF) preparation and cell counting. The lungs were lavaged three times with a total volume of 1.5 mL cold PBS followed by centrifugation at 700 g for 10 min at 4°C. The cell pellets were re-suspended in 1 mL PBS, and cell counting was performed using a hemocytometer in a double-blind manner. Differential cell counting was performed by Wright-Giemsa staining (KeyGen Biotech, Nanjing, China).

ELISAs

Peripheral blood samples were collected after 1, 2, 4, 6, 12, 24, and 72 h as well as one week of treatment (n = 5 per group at each time point). The concentrations of TNF-α, IL-1β, IL-8, IL-10, IL-17 and transforming growth factor (TGF)-β were determined using ELISA kits (Abcam, Cambridge, UK). The concentrations of Ang-2, VEGF, and ET-1 were determined using an ELISA kit from BioLegend, Inc. (San Diego, CA, USA). The optical density at 450 nm was measured, and the data were tabulated using GraphPad Prism 4.0 (GraphPad Software, Inc., San Diego, CA, USA).

Tissue processing

In the immediately treated group, both LPS- and L + C + A-treated rats were sacrificed at 1, 2, 4, 6, 12, 24, and 72 h as well as one week after LPS insult (n = 5 per group at each time point) under anesthesia with 0.75% intraperitoneal sodium pentobarbital (75 mg/g). While in the later treated group, L + C + A-treated rats were sacrificed at 6, 12, 24, 72 h and one week after LPS insult (n = 5 per time point). For histopathological examination, the trachea was cannulated with an indwelling needle and then perfused with saline followed by instillation with 4% paraformaldehyde in PBS for *in situ* fixation. Half of the lungs were incised and fixed in 4% paraformaldehyde for 4 h, followed by equilibrium in 30% sucrose solution in PBS. Frozen sections (20 μm thick) were prepared using a Leica cryostat and mounted on glass slides coated with 0.02% poly-L-lysine for histological analysis and immunofluorescent staining. The other half of lungs were fixed in 10% glutaraldehyde solution for transmission electron microscopy (EM) imaging.

Assessment of pulmonary vascular permeability by Evans blue extravasation

In each group, vascular permeability was assessed using a modified Evans blue extravasation method in 3 out of 15 rats. Briefly, anesthetized rats were infused with 2% Evans blue dye (in 0.9% normal saline, 4 mL/kg) at 37°C *via* the

right femoral vein over 5 min. The rats were then perfused with 300 mL saline to wash out any remaining dye in the blood vessels.

Wet-to-dry lung weight ratio (W/D ratio)

The rat lungs were dissected and weighed (wet weight) immediately following sacrifice ($n=5$). Then the tissues were dried in an 80°C incubator for 48 h and weighed (dry weight). The ratio of the wet lung weight to dry lung weight was calculated for assessment of lung edema.¹⁰

Histopathologic assessment of lung tissues

The lung tissue sections were prepared, stained with hematoxylin and eosin (H&E), and then observed under a light microscope by an experienced pathologist blinded to the experimental condition. The degree of lung injury was assessed by two independent pathologists blinded to the experimental conditions and scored as follows: 0, no injury; 1, edema/fibrin, hemorrhage (subpleural); 2, edema/fibrin, hemorrhage (interlobular); 3, edema/fibrin, hemorrhage (alveolar); 4, congestion of alveolar septa; and 5, hyaline membrane changes of alveolar septa. The score was averaged for each animal and compared among groups, resulting in a relative average score ranging from 0 to 1.¹²

Immunofluorescence and immunohistochemical staining

For immunofluorescence and immunohistochemical staining, slides were incubated with the following primary antibodies SP-C (1:500, AbCam, Cambridge, MA), CD68 and CD45 (1:100; Santa Cruz Biotechnology), CD31 (1:100; Santa Cruz Biotechnology), TNF- α (1:1000, ProSci Inc., Poway, CA, USA), α v β 3 (clone LM609, Chemicon, Euromedex, Souffelweyersheim, France), MPO (1:100; Santa Cruz Biotechnology, Santa Cruz, CA) overnight at 4°C. For immunofluorescent staining of MPO, CD31/ α v β 3, MPO, CD45, SP-C/CD68 and TNF- α staining, sections were rinsed with PBS three times followed by incubation with FITC/TRITC-conjugated secondary goat anti-rabbit/mouse IgG antibodies (1:200; Invitrogen, Carlsbad, CA) for 1 h at 37°C and mounted with Antifade Gel/Mount aqueous mounting media (Southern Biotech). Primary antibody controls were used to confirm IHC labeling specificity. The CD68+, TNF- α , and MPO+ cells were counted in randomly selected fields at 400 \times magnification (field radius = 225 μ m), and Image Pro Plus acquisition software (Media Cybernetics, Silver Spring, MD) was used to evaluate labeled cells in three visual fields per section.

EM

Fresh tissues were fixed in 10% glutaraldehyde and washed with 0.1 M PBS, followed by overnight postfixation in 1% osmium tetroxide at 4°C. Postfixed tissues were dehydrated by an ethanol gradient (30, 50, 70, 80, 90, 95%) for 5 min each, followed by three changes of 100% ethanol for 10 min each and then by two changes in 1,2-propylene oxide (PO) for 15 min each. Tissues were immersed in a PO:Epon mixture (1:1) for 1 h followed by embedding in

pure Epon, and then they were kept at 60°C for three days. Next, 90-nm-thick sections were prepared with a diamond knife on an ultracut microtome and collected on 200 mesh copper grids. The section-loaded grids were stained with lead citrate droplets and 8% uranyl acetate droplets for 20 min each in a Petri dish, followed by washing three times with distilled water. Finally, the grids were used for EM.

Western blotting

Rats were sacrificed by decapitation at 1, 2, 4, 6, 12, 24, and 72 h as well as one week ($n=4$). The tissue lysates were prepared as described previously.¹³ The protein was separated by 10% sodium dodecyl sulfate-polyacrylamide gel electrophoresis, followed by transfer to a polyvinylidene difluoride membrane. The membrane was blocked in 5% nonfat milk in Tris-buffered saline (TBST), followed by overnight incubation with rabbit antisera against TNF- α (1:1000; ProSci Inc.); TGF- β (1:800; Thermo Fisher Scientific), caspase-3 (1:1000; Cayman Chemical), CD68 (1:500; Santa Cruz Biotechnology), MPO (1:500; Santa Cruz Biotechnology, Santa Cruz, CA), and rabbit antiserum against β -actin (1:5000; Abcam) at 4°C. Then the membrane was washed with TBST, followed by incubation with peroxidase-conjugated secondary antibody for 1 h at room temperature. Protein bands were detected using a chemiluminescence (ECL) detection kit (GE Healthcare, Waltham, MA).

Statistical analyses

The data were analyzed using SPSS 13.0 software for Windows (SPSS, Inc., Chicago, IL, USA). Comparisons among the groups were performed using Student's *t*-test and one-way analysis of variance. A *p* value <0.05 was considered statistically significant.

Results

C16 and Ang-1 promote EC proliferation while suppressing monocyte migration across ECs in response to LPS *in vitro*

Since increased pulmonary vascular permeability is a prominent feature of ARDS, we sought to determine whether C16 and Ang-1 have a protective effect on endothelial barrier under inflammatory condition. As shown in Figure 1(a) and (b), LPS markedly inhibited HPMEC viability and proliferation, and dramatically promoted THP-1 cell transmigration across HPMECs, suggesting that LPS induces endothelial hyperpermeability. However, a combination of C16 and Ang-1 effectively reversed the effects of LPS on HPMECs and THP-1 cells (Figure 1(a) and (b)). The data show that treatment with C16 and Ang-1 decreases endothelial permeability in response to LPS *in vitro*, suggesting that C16 and Ang-1 may protect against vascular leakage in ARDS.

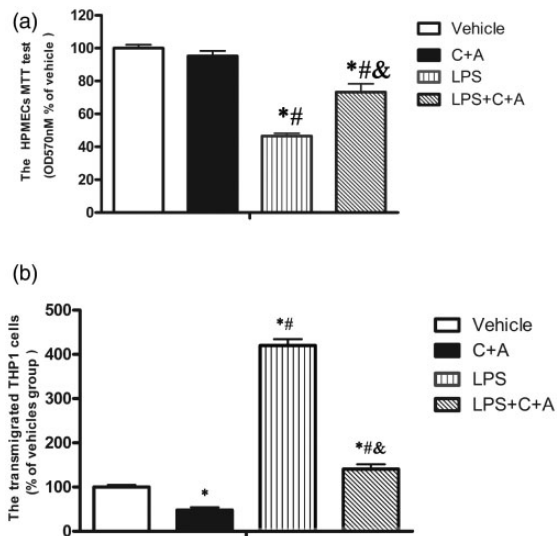


Figure 1. The effects of C16 and Ang-1 on endothelial permeability in response to LPS. LPS insult markedly inhibited HPMEC viability and proliferation as shown by MTT assay and dramatically promoted THP-1 cell transmigration across a HPMEC layer, suggesting LPS-induced endothelial hyperpermeability. However, a combination of C16 and Ang-1 effectively reversed the effects of LPS on the behavior of HPMECs and THP-1 cells. (a) MTT assay was performed to examine the effect of C16 and Ang-1 on HPMEC proliferation. (b) Transwell assay was performed to examine the effect of C16 + Ang-1 on THP-1 cell transmigration. The THP-1 cells within low chamber were counted. * $P < 0.05$ versus vehicle group, # $P < 0.05$ versus C + A group, & $P < 0.05$ versus LPS group. (Power calculation for differences between groups = 1 with group sizes per measurement = 5.)

HPMECs: human pulmonary microvascular endothelial cells; LPS: lipopolysaccharide; MTT: 3-(4,5)-dimethylthiaziazolo (-z-y1)-3,5-diphenyltetrazolium bromide; THP1: Human acute monocytic leukemia cell line.

C16 and Ang-1 inhibit LPS-induced death of HPMECs and HPAEpiCs in vitro

ARDS leads to pulmonary cell loss. We next sought to determine whether C16 and Ang-1 could protect cells from death in response to LPS. As shown in Figure 2, C16 and Ang-1 significantly inhibited LPS-induced necrosis in HPMECs and HPAEpiCs, as evidenced by the decreased percentage of number of necrotic marker PI-positive cells to total cells in LPS + C16 + Ang-1-treated HPMECs and HPAEpiCs, compared with LPS group (Figure 2(g) and (h)). These results indicate that C16 and Ang-1 inhibit LPS-induced necrosis in the pulmonary inflammatory response. Similarly, we also found that C16 and Ang-1 had a suppressive effect on LPS-induced apoptosis in HPMECs and HPAEpiCs (Figure 3), as evidenced by the decreased percentage of number of apoptotic marker caspase-3 positive cells to total cells in LPS + C16 + Ang-1-treated cells, respectively (Figure 3(g) and (h)). Collectively, our data demonstrate that C16 and Ang-1 inhibit LPS-induced death in HPMECs and HPAEpiCs, suggesting the possible role of C16 and Ang-1 in preventing tissue or cell loss in ARDS.

C16 and Ang-1 suppress LPS-induced inflammatory response in vitro

Because inflammatory response contributes to pathogenesis of LPS-induced ARDS, we investigated the role of C16 and Ang-1 in inhibition of LPS-induced inflammatory response. As shown in Figure 4(a) to (c), C16 and Ang-1 significantly suppressed LPS-induced secretion of pro-inflammatory cytokines IL-1 β , IL-8, and TNF- α from

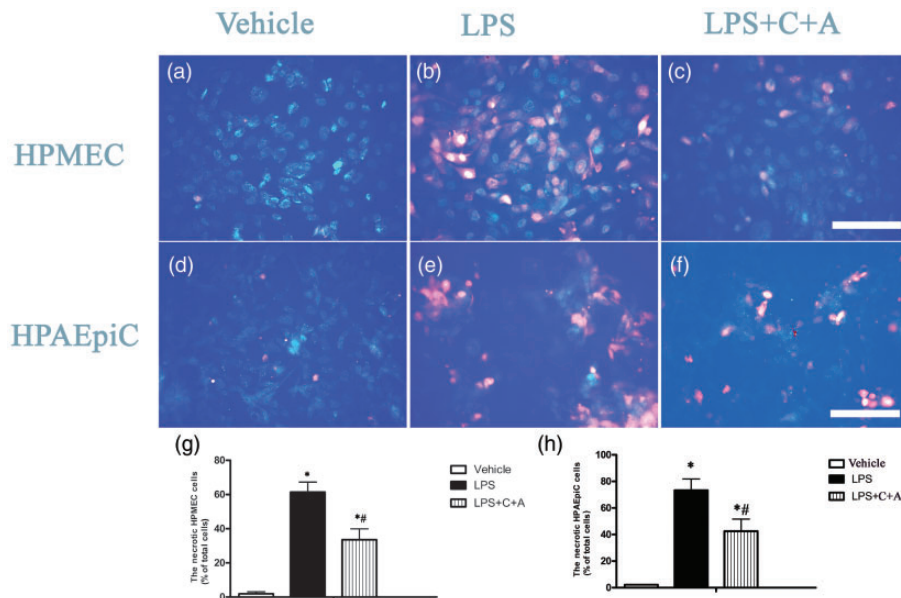


Figure 2. The inhibitory effects of C16 and Ang-1 on LPS-induced endothelial and epithelial necrosis. (a–f) Hoechst 33344 (blue)/PI (red) double staining was performed on HPMECs and HPAEpiCs for assessment of necrosis. Hoechst 33344 (blue) was used to stain nuclei and PI (red) was used to stain necrotic cells. In the vehicle group, necrotic cells were rarely found among either HPMECs or HPAEpiCs (a, d). LPS insult induced necrosis in endothelial (b) and epithelial (e) cells, and this effect was attenuated by C16 and Ang-1 treatment (c, f). The total numbers of cells and necrotic cells were counted in six randomly selected fields under 400 \times magnification in triplicate. The necrosis rate was calculated as the number of PI positive cells (red)/the number of total cells (blue) (g, h). Scale bar = 100 μ m. * $P < 0.05$ versus vehicle group, # $P < 0.05$ versus LPS group. (Power calculation for differences between groups = 1, group sizes per measurement = 5.) (A color version of this figure is available in the online journal.)

HPAEpiC: human pulmonary alveolar epithelial cell; HPMEC: human pulmonary microvascular endothelial cell; LPS: lipopolysaccharide.

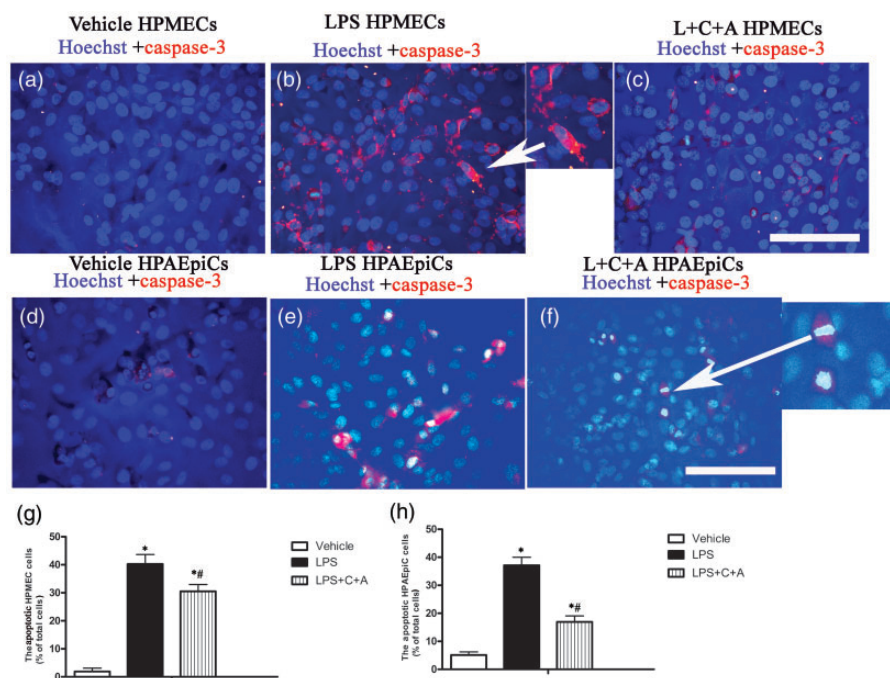


Figure 3. The inhibitory effects of C16 and Ang-1 on LPS-induced endothelial and epithelial apoptosis. (a–f) HPMECs and HPAEpiCs were double-immunostained with Hoechst 33342 (a fluorescent DNA dye, blue) and for cleaved caspase-3 (apoptotic cell marker, red). The Hoechst staining of nuclei showed that both HPMECs and HPAEpiCs formed monolayers, and the cleaved caspase-3-positive cells (indicated by arrows) in the partially magnified images in panels b and f, specifically depicted individual apoptotic cells. In the vehicle control, apoptotic cells were rarely found among HPMECs (a) or HPAEpiCs (d). LPS insult-induced apoptosis in endothelial (b) and epithelial (e) cells was suppressed by C16 and Ang-1 treatment (c, f). Scale bar = 100 μm. (g, h): The total number of cells (blue staining) and the number of apoptotic cells (red staining in cytoplasm) were counted in six randomly selected fields under 400× magnification. * $P < 0.05$ versus vehicle group, # $P < 0.05$ versus LPS group. (Power calculation for differences between groups = 1, group sizes per measurement = 5.) (A color version of this figure is available in the online journal.)

HPAEpiCs: human pulmonary alveolar epithelial cells; HPMECs: human pulmonary microvascular endothelial cells; LPS: lipopolysaccharide.

THP-1 cells, compared with LPS group (Figure 4(a) to (c)). Consistently, C16 and Ang-1 enhanced the secretion of anti-inflammatory cytokine IL-10 (Figure 4(d)). These results show that C16 and Ang-1 antagonize LPS-induced inflammatory response *in vitro*.

C16 and Ang-1 suppress LPS-induced pulmonary inflammatory response, inhibit pulmonary vascular permeability, and attenuate pulmonary edema *in vivo*

Inflammation plays a key role in the pathogenesis of ARDS. Notably, we found that administration of C16 and Ang-1 effectively reduced serum levels of IL-1 β , IL-8, and TNF- α as well as pro-inflammatory hormone ET-1 while elevating the serum level of IL-10 in LPS-induced ARDS rats for up to one week of treatment (Fig. 4E, F-Fig. 5A–C). In addition, C16 and Ang-1 also suppressed accumulation of inflammatory cells in BALF, as evidenced by reduced number of inflammatory cells including neutrophils and macrophages in BALF from C16 and Ang-1-treated ARDS rats (Fig. 5D and Supplementary Fig. 1). Taken together, the data indicate that C16 and Ang-1 have significant anti-inflammatory effects in response to LPS.

Moreover, C16 and Ang-1 treatment led to reductions in the serum levels of Ang-2 and VEGF, both of which are largely involved in the regulation of vascular permeability and pulmonary edema in ARDS (Fig. 5E and 5F).

The anti-inflammatory effects of C16 and Ang-1 were further confirmed by the decreased number of TNF- α -positive

cells (Fig. 6A, Supplementary Fig. 2); and downregulation of expression of TNF- α in lung tissues of C16 plus Ang-1-administered ARDS rats (Fig. 7a and 7b), especially in the early stage of treatment (1–12 h after the treatment). We subsequently investigated the role of C16 and Ang-1 in regulating pulmonary vascular permeability in ARDS rats. As shown in Fig. 6(b), C16 and Ang-1 significantly decreased the lung wet-to-dry lung weight ratio (W/D ratio) in LPS-induced ARDS rats. The protective effects of C16 and Ang-1 on pulmonary histology were further confirmed by a significantly decreased lung injury score following treatment with C16 and Ang-1 (Fig. 6c). Consistent with these findings, C16 and Ang-1 also effectively improved pulmonary ultrastructural features in ARDS rats, such as alveolar septal edema, inflammatory cells infiltration, and apoptotic/necrotic signs in type II alveolar epithelial cells (AECs) and blood vessels' ECs (Supplementary Fig. 3).

As shown in Supplementary Fig. 4, treatment with C16 and Ang-1 effectively decreased the number of MPO-positive cells in the alveolar space, suggesting an inhibition of neutrophil activity by C16 and Ang-1 (Fig. 6d; Fig. 7c, d; Supplementary Fig. 4). In addition, C16 and Ang-1 suppressed CD68-positive macrophage infiltration in alveolar space and septum in ARDS rats (Figures 6E and 7E–F). Collectively, our results demonstrate that treatment with C16 and Ang-1 can inhibit inflammatory cell infiltration in lung tissues of ARDS rats, suggesting an important role of C16 and Ang-1 in anti-inflammation in ARDS.

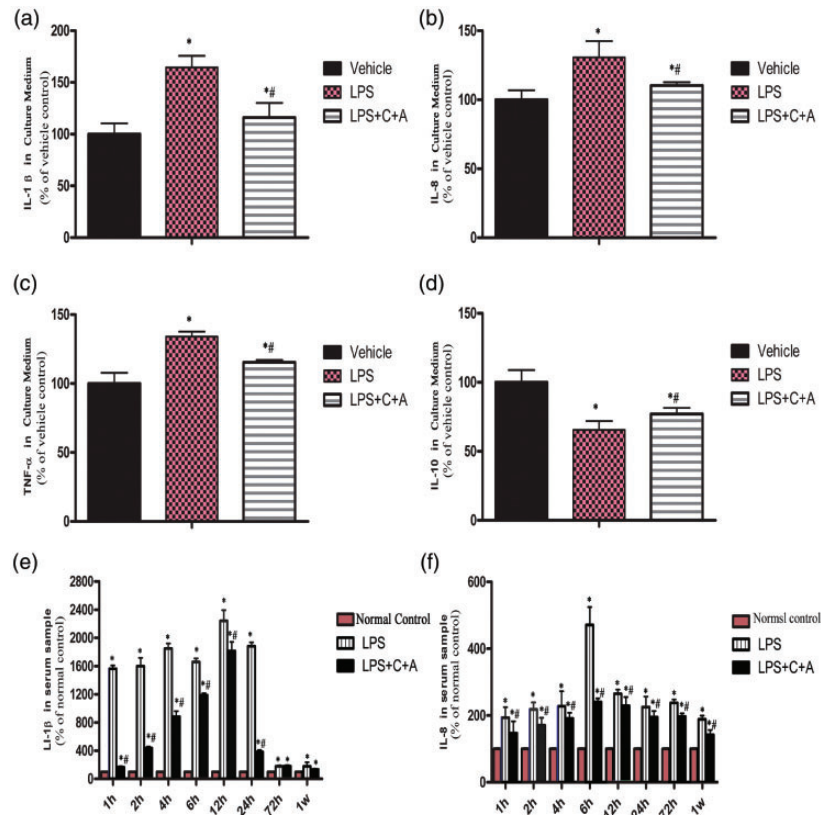


Figure 4. The suppressive effects of C16 and Ang-1 on the inflammatory factors and anti-inflammatory cytokine. (A-D) Levels of inflammatory mediators IL-1 β (A), IL-8 (B), TNF- α (C) and IL-10 (D) in THP-1 cell culture medium were measured using ELISA. * $P < 0.05$ vs. vehicle group, # $P < 0.05$ vs. LPS group (The results power calculation between each group = 1, group sizes per measurement = 5). (E-F) Serum levels of IL-1 β (E), IL-8 (F) in ARDS rats were measured using ELISA. (Panel E: The results power calculation of serum levels of IL-1 β between LPS and L+C+A group at 72 h post-insult = 0.357; at 1 week post-insult = 0.971. Panel F: The results power calculation of serum levels of IL-8 between LPS and L+C+A group at 12 h post-insult = 0.999; at 24 h post-insult = 0.989. Power calculation between other groups = 1, group sizes per measurement = 5).

IL: interleukin; LPS: lipopolysaccharide; TNF- α : tumor necrosis factor alpha.

C16 and Ang-1 diminish pulmonary fibrosis and apoptosis in LPS-induced ARDS rats

TGF- β is a multipotent cytokine closely associated with pulmonary fibrosis in ARDS. Our results revealed that treatment with C16 and Ang-1 effectively inhibited TGF- β expression in pulmonary parenchyma in LPS-induced ARDS rats (Figure 8A and 8B). Because pulmonary fibrosis correlates with apoptotic cell death in ARDS, we also investigated the effect of C16 and Ang-1 on pulmonary apoptosis. As shown in Fig. 8C and 8D, C16 and Ang-1 noticeably suppressed apoptotic marker caspase-3 expression in pulmonary interstitial and alveolar space in LPS-induced ARDS rats. Collectively, the data suggest that administration of C16 and Ang-1 may play a protective role in pulmonary fibrosis and apoptosis in ARDS.

C16 and Ang-1 increase survival and promote pulmonary gas exchange in LPS-induced ARDS rats

ARDS is a frequently lethal respiratory disease in which pulmonary gas exchange between alveoli and capillaries is severely impaired. We next sought to determine whether

C16 and Ang-1 treatment could protect ARDS rats from death and impaired pulmonary gas exchange. As shown in Fig. 9A, administration of C16 and Ang-1 led to a significant increase in survival rates in LPS-induced ARDS rats, especially in the late stage of the treatment. After one week of the C16 and Ang-1 treatment, the survival rate increased from 47% (7/15) to 80% (12/15) (Figure 9A). In addition, treatment with C16 and Ang-1 markedly decreased arterial carbon dioxide partial pressure (PCO₂) while increasing oxygen partial pressure (PO₂) in ARDS rats (Fig. 9B and 9C), thus enhancing arterial oxygen saturation (SO₂) (Fig. 9D). These data indicate that C16 and Ang-1 effectively promote pulmonary gas exchange and increase survival rates in LPS-induced ARDS rats.

C16 and Ang-1 attenuate lung injury in LPS-induced ARDS rats

We next sought to examine the effects of C16 and Ang-1 on pulmonary histology in ARDS rats. Given that enhancement in pulmonary vascular permeability allows the release of excess fluid into the interstitial space, leading to pulmonary edema, we also examined the effect of C16 and Ang-1 on pulmonary edema. The results indicated that C16

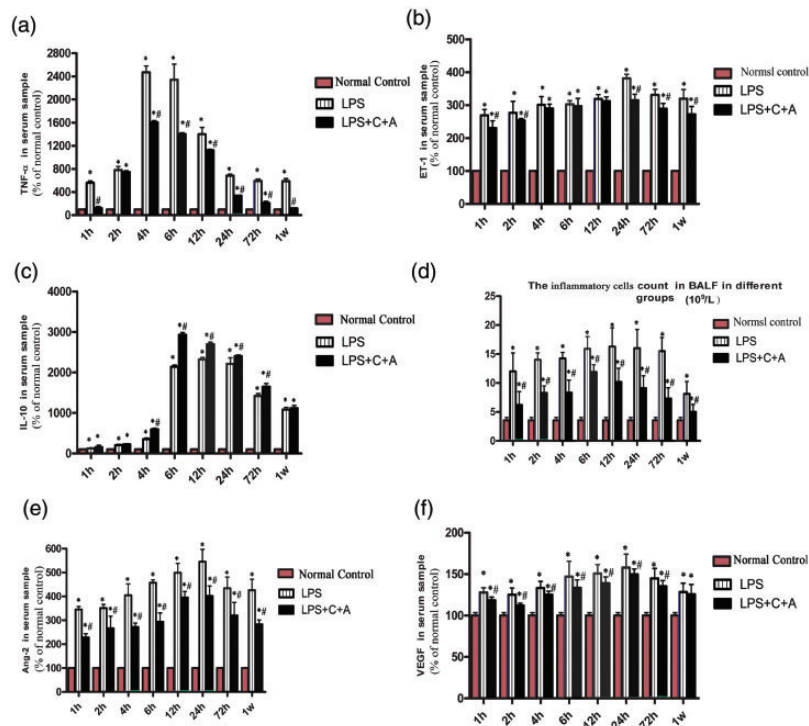


Figure 5. The effects of C16 and Ang-1 on the LPS-induced inflammatory response and corresponding promotion of anti-inflammatory cytokine IL-10 expression in vivo. (A-C) Serum levels of TNF- α (A), ET-1 (B) and IL-10 (C), in ARDS rats were measured using ELISA. (D) Inflammatory cell counting was performed in BALF showed C16 and Ang-1 treatment decreased inflammatory cell accumulation. (E-F) Moreover, C16 and Ang-1 treatment decreased the serum levels of Ang-2 (Fig. 5E) and VEGF in ARDS rats (Fig. 5F). * $P < 0.05$ vs. normal group, # $P < 0.05$ vs. LPS group (Panel A: The results power calculation of serum levels of TNF- α between normal control and L+C+A group at 1 h post-insult = 0.956; at 2 h post-insult = 0.946. Panel B: The results power calculation of serum levels of ET-1 between LPS and L+C+A group at 4 h post-insult = 0.414; at 6 h post-insult = 0.607; at 12 h post-insult = 0.463. Panel C: The results power calculation of serum levels of IL-10 between LPS and L+C+A group at 1 week post-insult = 0.527. Panel F: The results power calculation of serum levels of VEGF between LPS and L+C+A group at 1 week post-insult = 0.413. Power calculation between other groups = 1, group sizes per measurement = 5). Ang-1: angiotensin-1; BALF: bronchoalveolar lavage fluid; ET-1: endothelin-1; IL: interleukin; LPS: lipopolysaccharide; TNF- α : tumor necrosis factor alpha; VEGF: vascular endothelial growth factor.

and Ang-1 significantly suppressed pulmonary vascular permeability, as evidenced by a reduction in the intensity of Evans blue staining of pulmonary arteries in LPS-treated ARDS rats (Figure 10). Collectively, our results suggest that C16 and Ang-1 contribute to the maintenance of pulmonary vascular endothelial barrier integrity and alleviation of pulmonary edema in ARDS.

The results showed that treatment with C16 and Ang-1 greatly improved the pulmonary morphology in rats with LPS-induced ARDS, as evidenced by the marked reduction of pulmonary morphological abnormalities including vascular congestion, intravascular coagulation, alveolar edema and hemorrhage, and alveolar wall disruption (Supplementary Fig. 3). The MPO leukocytes infiltration, which can exert disastrous effects on pulmonary morphology, was also alleviated in C16 and Ang-1-treated ARDS rats (Supplementary Fig. 4). Moreover, even when initiated 6 h after LPS insult, C + A treatment still showed significant alleviating effects on pulmonary inflammatory cell infiltration at time points later than 6 h following LPS insult compared with the vehicle group, although the CD45⁺ leucocyte numbers also increased over time (Figure 11). Taken together, our data show that C16 and Ang-1 alleviated pulmonary structural and morphological injuries in rats with LPS-induced ARDS.

Discussion

ARDS, which is characterized by acute and progressive hypoxemic respiratory failure with bilateral pulmonary infiltrates, can be caused by multiple factors, such as severe sepsis, trauma, shock, burns, and inhaling harmful gas.¹⁴ Despite recent progress in pathophysiology, anesthesia, ventilatory support, antibiotic therapy, and critical care, the mortality rate of ARDS after pulmonary resections remains high at 40–60%. Early support of gas exchange with mechanical ventilation (MV) has been shown to be vital in the management of patients with ARDS. Moreover, respiratory distress syndrome is usually identified by changes in oxygenation, respiratory compliance, and lung water in clinical practice.^{15–16} In fact, arterial carbon dioxide tension (paCO₂), partial pressure of oxygen (PaO₂), and oxygen saturation (SaO₂) measured by a blood gas analyzer are important indexes in the diagnosis of ARDS and assessment of treatment efficacy.

In the clinical treatment of ARDS, ventilatory support has been shown to play a very important role in improving the PaO₂ and SaO₂ in the intensive care unit, and pharmacological interventions play accessory roles in increasing oxygenation. A plateau pressure <30 cmH₂O is recommended in all ARDS patients. Patients with moderate or

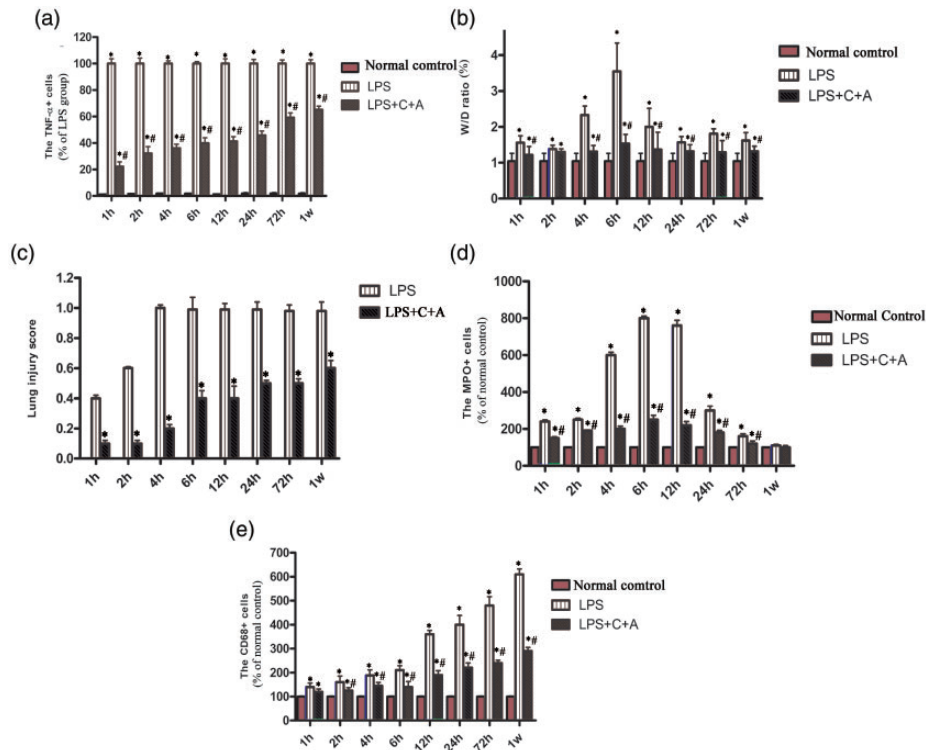


Figure 6. C16 and Ang-1 treatment had inhibitory effects on protein expression of inflammation-associated factors (A), lung edema (B), lung injury score (C), leukocyte infiltration (D-E). (A) TNF- α cell numbers were significantly increased in LPS treated group, which was evidently reversed in C+A treatment ($P < 0.05$). (B) The lung wet-to-dry weight ratio was compared among the normal control, LPS, and LPS+C16+Ang-1 groups. C16 and Ang-1 treatment reduced edema in lung tissue. * $P < 0.05$ vs. normal group, # $P < 0.05$ vs. LPS group. The lung wet-to-dry lung weight ratio was calculated as (Wet Weight - DryWeight)/Wet Weight $\times 100$. (C) The degree of lung injury was assessed in two slides per animal by two independent blinded pathologists and scored as follows: 0, no injury; 1, edema/fibrin, hemorrhage (subpleural); 2, edema/fibrin, hemorrhage (interlobular); 3, edema/fibrin, hemorrhage (alveolar); 4, congestion of alveolar septa; and 5, hyaline membrane changes of alveolar septa. (D) MPO+ cell numbers were increased 4–12 h after LPS insult, while the C+A treatment evidently inhibited MPO expression ($P < 0.05$). (E) CD68+ cell numbers were remarkably increased in the LPS group, especially at 3–7 days after LPS insult, while the C+A treatment still led to reduced CD68+ cell numbers ($P < 0.05$). Five sections were randomly selected, and images were photographed under $400\times$ magnification in three fields per section. Images of the staining for TNF- α (A), MPO (D), CD68 (E) were scanned and analyzed using NIH imaging software. * $P < 0.05$ vs. normal group, # $P < 0.05$ vs. LPS group. (Panel B: The results power calculation of W/D ratio between normal control and L+C+A group at 1 h post-insult = 0.95; at 4 h post-insult = 0.998; at 12 h post-insult = 0.999; at 24 h post-insult = 0.998; at 72 h post-insult = 0.910; at 1 week post-insult = 0.993. The results power calculation of W/D ratio between LPS and L+C+A group at 2 h post-insult = 0.856; at 4 h post-insult = 0.998; at 12 h post-insult = 0.998; at 24 h post-insult = 0.998; at 72 h post-insult = 0.998. Panel D: At 1 week post-insult, the results power calculation of MPO+ cell numbers between normal control and LPS group = 0.735; between normal control and L+C+A group = 0.658; between LPS and L+C+A group = 0.874. Panel E: The results power calculation of CD68+ cell numbers between LPS and L+C+A group at 1 h post-insult = 0.997; at 72 h post-insult = 0.998. Power calculation between other groups = 1, group sizes per measurement = 5) (A color version of this figure is available in the online journal.)

LPS: lipopolysaccharide; MPO+, myeloperoxidase; TNF- α : tumor necrosis factor alpha; W/D ratio: wet-to-dry lung weight ratio.

severe ARDS should receive higher levels of positive end-expiratory pressure.¹⁷

In the present study, PaO₂ and SaO₂ were significantly higher in the LPS + C + A group than in the LPS group. However, although statistically different, it has to be pointed out that these differences are too low to make a clinically relevant difference. In addition, bronchodilators, glucocorticosteroids (or drugs with similar effects), antibiotics, and oxygen in combination may be used in the treatment of ARDS.¹⁸ In fact, glucocorticosteroid therapy alone showed a minimal effect on reducing PaO₂ in treatment of ARDS, although it has been shown to reduce the infiltration of inflammatory cells and inhibit the formation of hyaline membranes.¹⁹

In ARDS, direct or indirect pulmonary insults cause alveolar and capillary endothelial damage, leading to the disruption of the vascular integrity, pulmonary leukocyte accumulation, edema, severe inflammation, and even death.²⁰ To facilitate the study of the molecular mechanisms

underlying ARDS, animal models of ARDS have been established including LPS administration, hyperoxia, and MV. Among them, LPS administration is the most commonly used approach to mimicking ARDS by inducing sepsis, a major cause of ARDS.¹³

Like ARDS, sepsis-induced lung injury is characterized by activation of vascular ECs and increased leukocyte-EC adhesion, migration and infiltration of neutrophils to the lungs, as well as enhanced secretion of pro-inflammatory mediators.^{13,21}

Previous studies have shown LPS dose-dependently induces leukocyte-vascular EC adhesion both *in vivo* and *in vitro*, thus initiating an early inflammatory response.^{21–23} LPS also promotes apoptosis in the AECs.²⁴

In this study, our results showed that LPS treatment disrupted the blood-alveolar barrier, leading to pulmonary edema. A combination of C16 and Ang-1 preserved the relatively normal structure and function in spite of the destructive effects of LPS on ECs and AECs *in vitro*, as

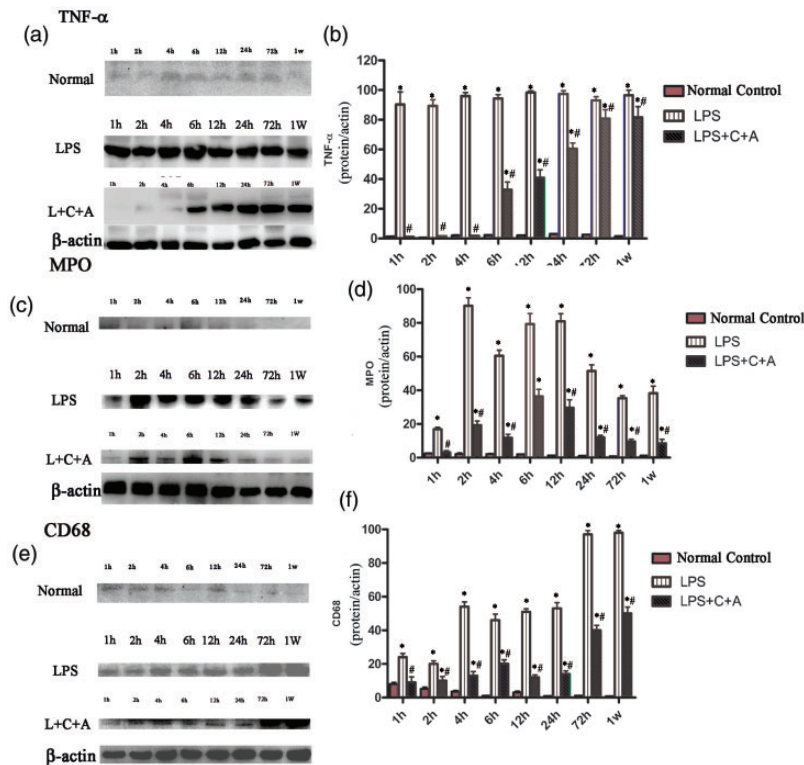


Figure 7. The suppressive effects of C16 and Ang-1 on protein expression of inflammation-associated factors in vivo. Western blot assays were performed to examine the expression of inflammation-associated factors and leukocyte infiltration as indicated in lung tissues of ARDS rats. β -actin was used as an internal control. Treatment with C16 and Ang-1 suppressed the expression of the inflammatory cytokine TNF- α (A, B), neutrophil specific marker MPO (at early stage following insult, C, D) and the expression levels of leukocyte marker CD68 (at late stage following insult, E, F) as well as were all significantly increased after LPS insult, whereas C+A treatment obviously inhibited these increases in protein expression. Quantification of Western blot data by normalization to β -actin expression. * $P < 0.05$ vs. normal group, # $P < 0.05$ vs. LPS group (Panel B: The results power calculation of TNF- α expression between normal control and L+C+A group at 1 h post-insult = 0.051; at 4 h post-insult = 0.999. Panel D: The results power calculation of MPO expression between Normal control and L+C+A group at 1 h post-insult = 0.943. Panel F: The results power calculation of CD68 expression between normal control and L+C+A group at 1 h post-insult = 0.408. Power calculation between other groups = 1, group sizes per measurement = 5).

well as prevented ARDS by decreasing the blood vessel leakage, suggesting the protective role of C16 and Ang-1 in the blood-alveolar barrier, which was further confirmed by the *in vivo* data in the study.

LPS induced expression and secretion of pro-inflammatory mediators including TNF- α , IL-1 β , and IL-8, as shown by their elevated levels in the serum and BALF of LPS-induced ARDS rats. These inflammatory mediators are strongly involved in the pathogenesis of ARDS, contributing to the severity of lung injury.^{25–28} TNF- α and IL-1 β are early response cytokines produced by activated alveolar macrophages and play a central role in developing pulmonary edema and mediating alveolar epithelial dysfunction,^{25–28} whereas upregulation of IL-8 is usually correlated with poor prognosis in sepsis patients.²⁷ The pathophysiology of ARDS includes an overlap between acute “inflammatory” and delayed “repair/fibrotic” phases. TGF- β contributes to the pathogenesis of ARDS by stimulating fibroblast proliferation, thus leading to the development of pulmonary fibrosis.^{29,30} Our results showed that C16 and Ang-1 significantly inhibited the production and secretion of TNF- α , IL-1 β , and IL-8 and TGF- β *in vitro* and *in vivo*, suggesting that the anti-

inflammatory effect of C16 and Ang-1 is associated with their inhibition of cytokine production and fibrotic process. As an anti-inflammatory cytokine, IL-10 has been reported to inhibit LPS-mediated production of TNF- α and IL-1 β in myeloid lineage cells.^{31,32} In our study, C16 and Ang-1 treatment significantly upregulated IL-10 levels. The inhibition of IL-1 β , IL-8, and TNF- α expression by C16 and Ang-1 may be at least partially attributed to the upregulation of IL-10.

An increased number of leukocytes in the blood are a prominent feature of bacterial sepsis. As we demonstrated, MPO-positive neutrophil infiltration appears initially after LPS insult, followed by CD68-positive macrophage accumulation in the lesion. When circulating neutrophils become primed, they migrate across the endothelium, interstitium, and epithelium into the air spaces where they release oxidants, proteases, and neutrophil extracellular traps to kill invading pathogens.³³ In ARDS, neutrophils and their toxic mediators increase lung endothelial and epithelial permeability, resulting in alveolar edema and arterial hypoxemia.³³ Therefore, targeting neutrophils, which can reduce pulmonary vascular endothelial permeability and promote alveolar epithelial integrity, may be a potential therapeutic strategy against ARDS.

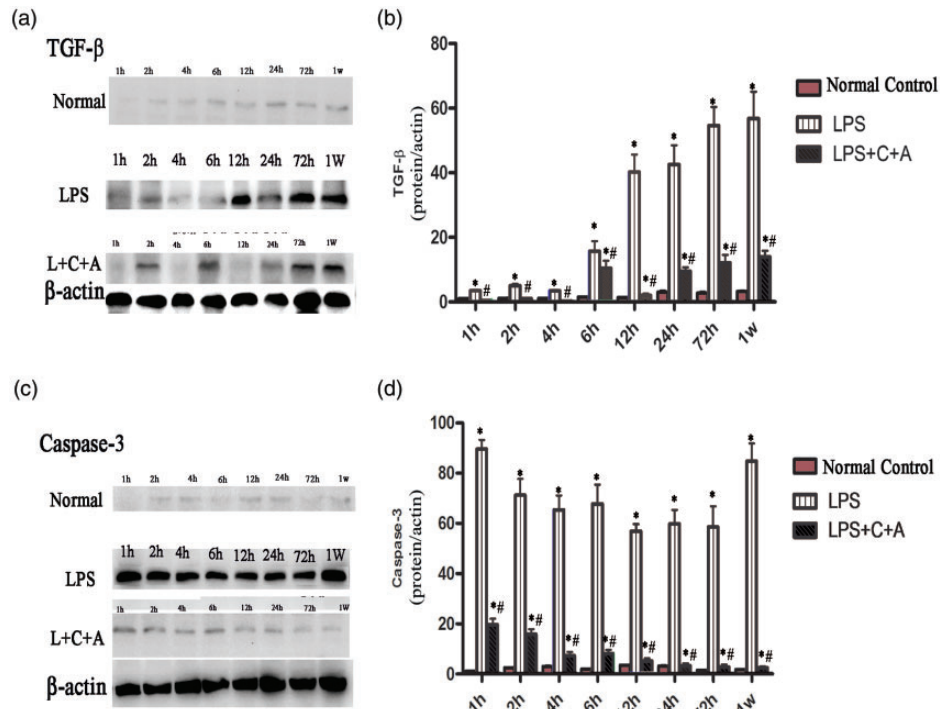


Figure 8. The suppressive effects of C16 and Ang-1 on protein expression of pulmonary fibrotic factor TGF- β and apoptotic marker cleaved caspase-3. Quantification of Western blot data by normalization to β -actin expression. * $P < 0.05$ vs. normal group, # $P < 0.05$ vs. LPS group (Panel B: The results power calculation of TGF- β expression between normal control and L+C+A group at 2 h post-insult = 0.831. Panel J: The results power calculation of activated Caspase-3 expression between normal control and L+C+A group at 24 h post-insult = 0.062; at 72 h post-insult = 0.987. Power calculation between other groups = 1, group sizes per measurement = 5). LPS: lipopolysaccharide; TGF- β : Transforming growth factor.

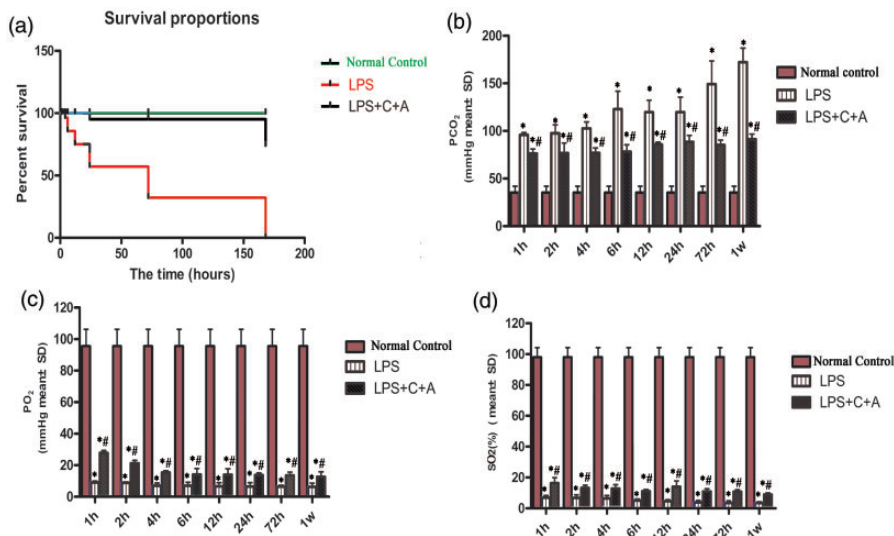


Figure 9. Improved survival and pulmonary gas exchange in ARDS rats after C16 and Ang-1 treatment. (A) Survival data in LPS-induced ARDS rats of each group. * $P < 0.05$ vs. normal group, # $P < 0.05$ vs. LPS group ($n = 15$). (B-D) Arterial carbon dioxide and oxygen partial pressure as well as arterial oxygen saturation were measured using a blood gas analyzer. * $P < 0.05$ vs. normal group, # $P < 0.05$ vs. LPS group. (Power calculation between other each group = 1, group sizes per measurement = 15).

C16 peptide has integrin-mediated anti-inflammatory activity, which has been confirmed in animal models of neuromyelitis optica³⁴ and autoimmune encephalomyelitis.^{4,6-8} It is known that integrins $\alpha v \beta 3$ and $\alpha 5 \beta 1$ are the surface receptors of C16. The $\alpha v \beta 3$ integrin plays a key

role in leukocyte migration since it provides an interaction site for both leukocyte directional locomotion and formation of the leukocyte-endothelial synapse. In this study, $\alpha v \beta 3$ was substantially expressed on cultured HPMECs (Supplementary Fig. 4S). C16 could competitively interfere

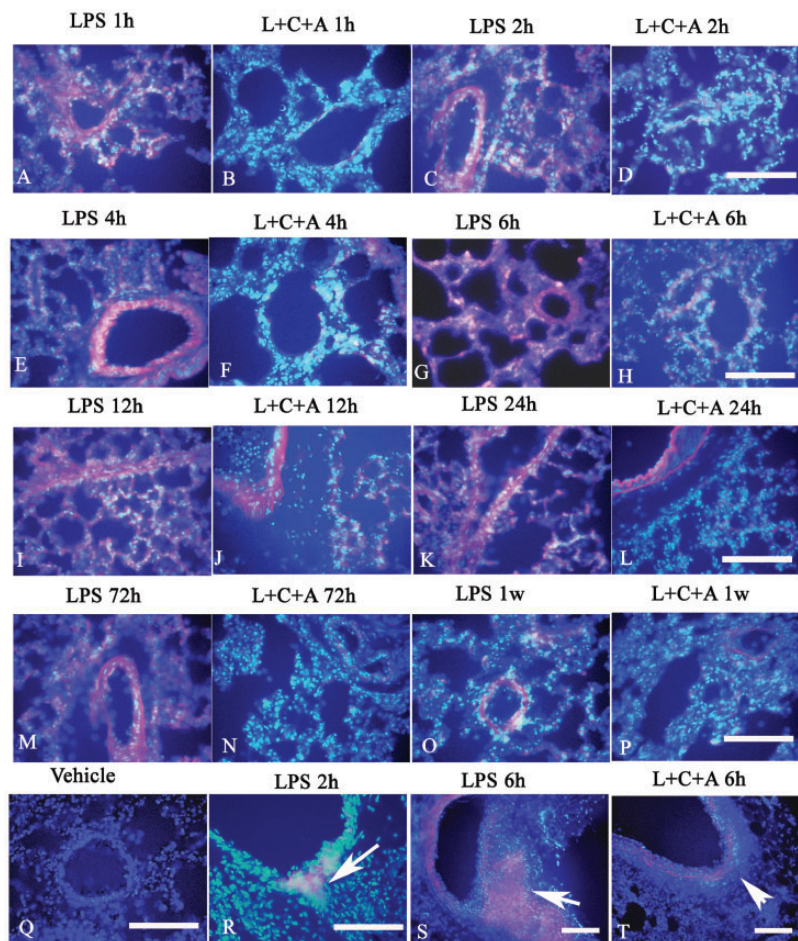


Figure 10. The inhibitory effects of C16 and Ang-1 on pulmonary vascular permeability and edema in ARDS rats. (A–Q) Assessment of Evans blue (EB) extravasation in LPS-induced ARDS rats ($n = 3$). EB extravasations assay was performed to observe the pulmonary vascular permeability. EB staining was visualized via red laser excitation at 405nm. Without the EB leakage, the pulmonary tissue appeared light blue due to autofluorescence of the tissue, as shown in the normal control in Q. The tissue color turned red (A, C, E, G, I, J, K, M, O) due to medium or high vascular permeability. However, if there is no or only low vascular permeability, only the small amount of tissue that contacts EB will turn to red (B, D, F, H, L, N, P). The arrow in panel R points to where the EB was leaking from the blood vessel, and the arrow in panel S shows that a great amount of EB (red color) has bled out from a blood vessel. However, at the same time point, the blood vessel in the C16 and Ang-1–treated group did not exhibit clear EB leakage, as indicated by the arrow in panel T. Scale bar = 100 μm . (A color version of this figure is available in the online journal)

with the binding of a leukocyte ligand to the endothelium and thus competitively prevent leukocyte transmigration *via* high affinity binding to $\alpha v\beta 3$.

Ang-1 is a ligand of the endothelial receptor Tie2 and protects the vasculature from plasma leakage induced by inflammatory stimuli.⁵ Ang-1 and Ang-2 exert opposite effects on edema and inflammation³⁵ through binding to a common receptor Tie2, and thus, they antagonize each other to control blood vessel maturation and stabilization. Ang-1 stabilizes blood vessel formation, whereas Ang-2 destabilizes the blood vessel structure and increases vascular permeability in lung injury.³⁶ Previous studies have showed that in ARDS, plasma Ang-2 outperforms other markers and the elevated plasma level of Ang-2 between days 1 and 3 is strongly associated with mortality.³⁷ Ang-2 can lead to endothelial dysregulation and endothelial damage, exacerbating lung edema.³⁵ In a previous study, Ang-1 treatment generated an antagonistic effect on the Ang-2 level *via* the PI3K/Akt pathway.³⁸ Furthermore, the

treatment also downregulated the tissue expression and serum level of VEGF, a potential regulator of vascular permeability, in ARDS rats.^{39,40}

Like TNF- α , IL-1 β , and IL-8, ET-1 is also recognized as a pro-inflammatory mediator in ARDS. Ang-1 has been found to have a suppressive effect on ET-1 expression.⁴¹ A combination of C16 and Ang-1 thus may have a much higher therapeutic value for ARDS than C16 or Ang-1 alone due to synergistic action between them, although the protective effects of Ang-1 and C16 partially overlap.

The LPS-induced alterations were restored between 6 and 24 h following LPS injection. Notably, the C + A-treated group continued to exhibit significant alleviation compared with the vehicle control at the same time point ($P < 0.05$), suggesting that the treatment was still effective. Furthermore, C + A treatment, when implemented 6 h following LPS injection, showed significant alleviating effects on pulmonary leukocyte infiltration at time points later than 6 h following LPS insult.

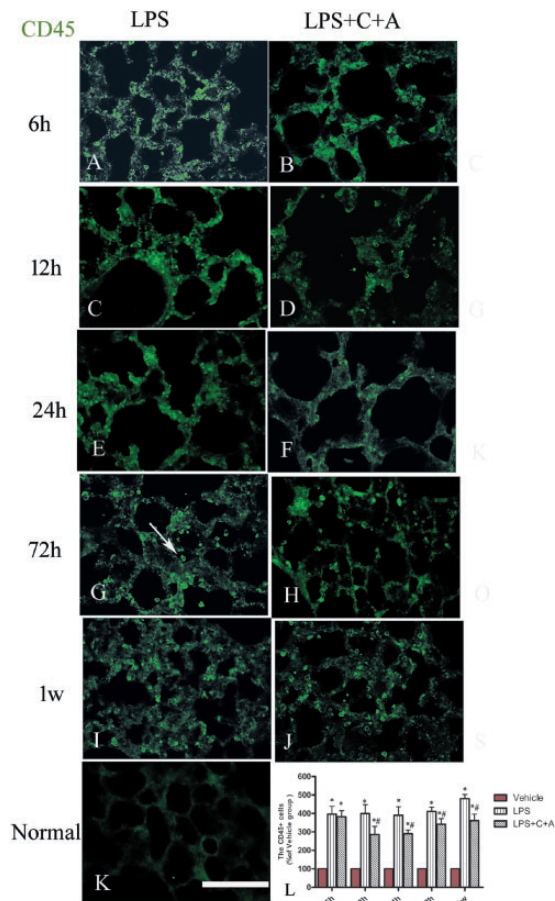


Figure 11. Effect of C16 and Ang-1 on macrophage infiltration in rats with the treatment given 6 h post-LPS insult. (a–k) Immunohistochemical staining for CD45 (green) in lung tissues of rats with LPS-induced ARDS. In the normal control, there was no obvious macrophage infiltration in pulmonary tissue (k). At 6 h after the insult, in both the PBS-treated LPS group (a) and C + A-treated group (b), many CD45+ leucocytes were observed in lung tissue. However, from 12 h after the insult, the C + A treatment (d, f, h, j) showed visible alleviating effects on pulmonary inflammatory cell infiltration compared with the PBS-treated group (c, e, g, i), although leucocyte infiltration in both groups gradually increased with time. The white arrow in panel g points to a typical CD45-labeled leucocyte. The calculation CD45+ cell numbers are shown in panel l. Scale bar = 100 μ m (n = 5). (A color version of this figure is available in the online journal.)
LPS: lipopolysaccharide.

Furthermore, the beneficial effects were sustainable, remaining active after the termination of the treatment at one week postinsult. These results also suggest that C16 and Ang-1, when combined, could have potential additive and lasting effects.

Conclusions

In conclusion, our study has demonstrated functional and morphological abnormalities in lung tissues of LPS-induced ARDS rats, and that combined administration of C16 and Ang-1 significantly protected lung tissue from abnormal changes in structure and function after LPS insult. Based on the novel findings in ARDS rats, the potential value of C16 and Ang-1 in combination in the treatment of inflammatory lung diseases warrants further investigation.

Authors' contributions: SH and MZ contributed equally to this paper. SH and MZ designed the experiments and drafted the manuscript; QL and LGY participated in the study design and coordination; YYZ, XXF, and DQW performed the experiments; YYZ, XXF, and DQW analyzed the data and revised the manuscript. All authors read and approved the final manuscript.

DATA AVAILABILITY

The datasets used and/or analyzed during the current study are available from the corresponding author on reasonable request.

DECLARATION OF CONFLICTING INTERESTS

The author(s) declared no potential conflicts of interest with respect to the research, authorship, and/or publication of this article.

FUNDING

The author(s) disclosed receipt of the following financial support for the research, authorship, and/or publication of this article: This work was supported by the Zhejiang Provincial Natural Science Foundation of China (grant no. LY17H150001) and Zhejiang Medical and Health Science and Technology Project (grant no. 2017195219) and Project of Technology Consultant (grant no. 519000-I41701).

ORCID iD

Shu Han  <https://orcid.org/0000-0002-7800-2394>

REFERENCES

- Liu N, Liu X, Li X, Duan K, Deng Y, Yu X, Peng Q. DOK3 degradation is required for the development of LPS-induced ARDS in mice. *Curr Gene Ther* 2016;**16**:256–62
- Fodor RS, Georgescu AM, Cioc AD, Grigorescu BL, Cotoi OS, Fodor P, Copotoiu SM, Azamfirei L. Time- and dose-dependent severity of lung injury in a rat model of sepsis. *Rom J Morphol Embryol* 2015;**56**:1329–37
- Kumpers P, Lukasz A. The curse of angiotensin-2 in ARDS: on stranger TI(E)des. *Crit Care* 2018;**22**:44
- Jiang H, Zhang F, Yang J, Han S. Angiotensin-1 ameliorates inflammation-induced vascular leakage and improves functional impairment in a rat model of acute experimental autoimmune encephalomyelitis. *Exp Neurol* 2014;**261**:245–57
- Han S, Arnold SA, Sithu SD, Mahoney ET, Geraldts JT, Tran P, Benton RL, Maddie MA, D'Souza SE, Whittemore SR, Hagg T. Rescuing vasculature with intravenous angiotensin-1 and alpha v beta 3 integrin peptide is protective after spinal cord injury. *Brain* 2010;**133**:1026–42
- Fang M, Sun Y, Hu Z, Yang J, Davies H, Wang B, Ling S, Han S. C16 peptide shown to prevent leukocyte infiltration and alleviate detrimental inflammation in acute allergic encephalomyelitis model. *Neuropharmacology* 2013;**70**:83–99
- Zhang F, Yang J, Jiang H, Han S. An alphanubeta3 integrin-binding peptide ameliorates symptoms of chronic progressive experimental autoimmune encephalomyelitis by alleviating neuroinflammatory responses in mice. *J Neuroimmune Pharmacol* 2014;**9**:399–412
- Han S, Zhang F, Hu Z, Sun Y, Yang J, Davies H, Yew DT, Fang M. Dose-dependent anti-inflammatory and neuroprotective effects of an alpha-nubeta3 integrin-binding peptide. *Mediators Inflamm* 2013;**2013**:268486
- Fang M, Wang J, Zhang X, Geng Y, Hu Z, Rudd JA, Ling S, Chen W, Han S. The miR-124 regulates the expression of BACE1/beta-secretase

- correlated with cell death in Alzheimer's disease. *Toxicol Lett* 2012;**209**:94–105
10. Qi D, Wang D, Zhang C, Tang X, He J, Zhao Y, Deng W, Deng X. Vaspin protects against LPS induced ARDS by inhibiting inflammation, apoptosis and reactive oxygen species generation in pulmonary endothelial cells via the akt/GSK3beta pathway. *Int J Mol Med* 2017;**40**:1803–17
 11. Ding Q, Liu GQ, Zeng YY, Zhu JJ, Liu ZY, Zhang X, Huang JA. Role of IL-17 in LPS-induced acute lung injury: an in vivo study. *Oncotarget* 2017;**8**:93704–11
 12. Haque A, Scultetus AH, Arnaud F, Dickson LJ, Chun S, McNamee G, Auken CR, McCarron RM, Mahon RT. The emulsified PFC oxycyte((R)) improved oxygen content and lung injury score in a swine model of oleic acid lung injury (OALI). *Lung* 2016;**194**:945–57
 13. Jin B, Jin H. Oxymatrine attenuates lipopolysaccharide-induced acute lung injury by activating the epithelial sodium channel and suppressing the JNK signaling pathway. *Exp Anim* 2018;**67**:337–47
 14. Fu H, Sun M, Miao C. Effects of different concentrations of isoflurane pretreatment on respiratory mechanics, oxygenation and hemodynamics in LPS-induced acute respiratory distress syndrome model of juvenile piglets. *Exp Lung Res* 2015;**41**:415–21
 15. Mancini M, Zavala E, Mancebo J, Fernandez C, Barberà JA, Rossi A, Roca J, Rodriguez-Roisin R. Mechanisms of pulmonary gas exchange improvement during a protective ventilatory strategy in acute respiratory distress syndrome. *Am J Respir Crit Care Med* 2001;**164**:1448–53
 16. Mehaffey JH, Charles EJ, Schubert S, Salmon M, Sharma AK, Money D, Stoler MH, Laubach VE, Tribble CG, Roeser ME, Kron IL. In vivo lung perfusion rehabilitates sepsis-induced lung injury. *J Thorac Cardiovasc Surg* 2018;**155**:440–8.e2
 17. Bos LD, Martin-Loeches I, Schultz MJ. ARDS: challenges in patient care and frontiers in research. *Eur Respir Rev* 2018;**27**:170107
 18. Liu J, Rc C, Zhong NS. Application of capnography and SpO₂ measurement in the evaluation of respiratory failure in patients with chronic obstructive pulmonary disease. *Nan Fang Yi Ke Da Xue Xue Bao* 2010;**30**:1565–8
 19. Häfner D, Germann PG. Dexamethasone enhances the activity of rSP-C surfactant but not of exosurf in a rat model of the acute lung injury. *J Pharmacol Toxicol Methods* 1999;**42**:39–48
 20. Fan EKY, Fan J. Regulation of alveolar macrophage death in acute lung inflammation. *Respir Res* 2018;**19**:50
 21. Wu YH, Chuang SY, Hong WC, Lai YJ, Chang GJ, Pang JH. Berberine reduces leukocyte adhesion to LPS-stimulated endothelial cells and VCAM-1 expression both in vivo and in vitro. *Int J Immunopathol Pharmacol* 2012;**25**:741–50
 22. Mitra S, Wewers MD, Sarkar A. Mononuclear phagocyte-derived microparticulate caspase-1 induces pulmonary vascular endothelial cell injury. *PLoS One* 2015;**10**:e0145607
 23. Zhang K, Wang P, Huang S, Wang X, Li T, Jin Y, Hehr M, Xu C. Different mechanism of LPS-induced calcium increase in human lung epithelial cell and microvascular endothelial cell: a cell culture study in a model for ARDS. *Mol Biol Rep* 2014;**41**:4253–9
 24. Hecker M, Behnk A, Morty RE, Sommer N, Vadasz I, Herold S, Seeger W, Mayer K. PPAR-alpha activation reduced LPS-induced inflammation in alveolar epithelial cells. *Exp Lung Res* 2015;**41**:393–403
 25. Patel BV, Wilson MR, O'Dea KP, Takata M. TNF-induced death signaling triggers alveolar epithelial dysfunction in acute lung injury. *J Immunol* 2013;**190**:4274–82
 26. Peng J, Wei D, Fu Z, Li D, Tan Y, Xu T, Zhou J, Zhang T. Punicalagin ameliorates lipopolysaccharide-induced acute respiratory distress syndrome in mice. *Inflammation* 2015;**38**:493–9
 27. Hendrickson CM, Matthay MA. Endothelial biomarkers in human sepsis: pathogenesis and prognosis for ARDS. *Pulm Circ* 2018;**8**:2045894018769876
 28. Aisiku IP, Yamal JM, Doshi P, Benoit JS, Gopinath S, Goodman JC, Robertson CS. Plasma cytokines IL-6, IL-8, and IL-10 are associated with the development of acute respiratory distress syndrome in patients with severe traumatic brain injury. *Crit Care* 2016;**20**:288
 29. Frank JA, Matthay MA. TGF-beta and lung fluid balance in ARDS. *Proc Natl Acad Sci USA* 2014;**111**:885–6
 30. Deng X, Jin K, Li Y, Gu W, Liu M, Zhou L. Platelet-derived growth factor and transforming growth factor beta1 regulate ARDS-Associated lung fibrosis through distinct signaling pathways. *Cell Physiol Biochem* 2015;**36**:937–46
 31. Opp MR, Smith EM, Hughes TK Jr. Interleukin-10 (cytokine synthesis inhibitory factor) acts in the central nervous system of rats to reduce sleep. *J Neuroimmunol* 1995;**60**:165–8
 32. Hu Y, Qin C, Zheng G, Lai D, Tao H, Zhang Y, Qiu G, Ge M, Huang L, Chen L, Cheng B, Shu Q, Xu J. Mesenchymal stem cell-educated macrophages ameliorate LPS-Induced systemic response. *Mediators Inflamm* 2016;**2016**:3735452
 33. Zemans RL, Matthay MA. What drives neutrophils to the alveoli in ARDS? *Thorax* 2017;**72**:1–3
 34. Zheng X, Zhang W, Hu X. Different concentrations of lipopolysaccharide regulate barrier function through the PI3K/akt signalling pathway in human pulmonary microvascular endothelial cells. *Sci Rep* 2018;**8**:9963
 35. Milam KE, Parikh SM. The angiotensin-Tie2 signaling axis in the vascular leakage of systemic inflammation. *Tissue Barriers* 2015;**3**:e957508
 36. Mammoto T, Jiang A, Jiang E, Mammoto A. Platelet-rich plasma extract prevents pulmonary edema through angiotensin-Tie2 signaling. *Am J Respir Cell Mol Biol* 2015;**52**:56–64
 37. Zinter MS, Spicer A, Orwoll BO, Alkhouli M, Dvorak CC, Calfee CS, Matthay MA, Sapru A. Plasma angiotensin-2 outperforms other markers of endothelial injury in prognosticating pediatric ARDS mortality. *Am J Physiol Lung Cell Mol Physiol* 2016;**310**:L224–31
 38. Tsigkos S, Zhou Z, Kotanidou A, Fulton D, Zakynthinos S, Roussos C, Papapetropoulos A. Regulation of Ang2 release by PTEN/PI3-kinase/akt in lung microvascular endothelial cells. *J Cell Physiol* 2006;**207**:506–11
 39. Kosmidou I, Karpaliotis D, Kirtane AJ, Barron HV, Gibson CM. Vascular endothelial growth factors in pulmonary edema: an update. *J Thromb Thrombolysis* 2008;**25**:259–64
 40. Guo Q, Yuan JJ, Zeifman JX, Chen A, Shen J, Huang B, Vegf J. Bcl-2 and bad regulated by angiotensin-1 in oleic acid induced acute lung injury. *Biochem Biophys Res Commun* 2011;**413**:630–6
 41. McCarter SD, Lai PF, Suen RS, Stewart DJ. Regulation of endothelin-1 by angiotensin-1: implications for inflammation. *Exp Biol Med* 2006;**231**:985–91

(Received March 15, 2020, Accepted August 7, 2020)